Effects of Electronic Structures on the Excited-State Intramolecular Proton Transfer of 1-Hydroxy-2-acetonaphthone and Related Compounds

Seiji Tobita,* Masataka Yamamoto, Noriko Kurahayashi, Rie Tsukagoshi, Yosuke Nakamura, and Haruo Shizuka*

Department of Chemistry, Gunma University, Kiryu, Gunma 376-8515, Japan

Received: March 4, 1998; In Final Form: April 24, 1998

Effects of electronic structures on the excited-state intramolecular proton transfer (ESIPT) of 1-hydroxy-2-acetonaphthone (1H2AN) and its related compounds [1-hydroxy-2-naphthaldehyde (1H2NA) and methyl 1-hydroxy-2-naphthoate (1H2MN)] were studied by means of the laser photolysis method, time-resolved thermal lensing technique, and fluorometry. Both 1H2AN and 1H2NA showed relatively large Stokes-shifted fluorescence ($\Delta\bar{\nu}$ = 6120 and 6170 cm^{-1}, respectively) and strongly temperature-dependent fluorescence observed usually for ESIPT systems. In contrast, the fluorescence properties of 1H2MN gave no indication of the occurrence of ESIPT. A 355 nm laser photolysis of 1H2AN or 1H2NA in cyclohexane produced a ground-state transient. The decay rate of the transient was markedly enhanced by addition of alcohols or triethylamine in nonpolar aprotic solvents. Furthermore, a bimolecular decay process probably due to mutual hydrogen exchange in a hydrogen-bonded complex was found for the transient from laser intensity dependence of the decay profiles. These observations could be reasonably explained by the occurrence of ESIPT in 1H2AN and 1H2NA to form a long-lived keto-tautomer. The distinct relaxation properties of excited 1H2AN and 1H2NA from that of 1H2MN were attributable to differences in relative stabilities between parent enol- and tautomeric keto-forms in the lowest excited singlet state, which are strongly affected by the electronic effects of the substituent on the carbonyl group.

1. Introduction

It has been well-known that excited-state intramolecular proton (or hydrogen atom) transfer (ESIPT) often plays a dominant role in the photorelaxation processes of intramolecularly hydrogen bonded molecules because of its ultrafast nature.[1−6] Since the original work of Weller[7] on the ESIPT of methyl salicylate (MS), a large number of experimental[8−15] and theoretical[16−22] studies on the ESIPT of a variety of systems have been reported. Among them, MS[23−32] and its related compounds, *o*-hydroxyacetophenone (OHAP)[33−35] and *o*-hydroxybenzaldehyde (OHBA),[36−39] have been well studied as prototypes of the molecules showing the ESIPT process. The electronic-state dependence of the intramolecular proton transfer of OHBA in the vapor phase has been studied by Nagaoka et al.[17,18] They proposed a new description of the occurrence of ESIPT on the basis of the nodal pattern of the wave function of the molecule. Herek et al.[25] reported that excited MS in an isolated state undergoes intramolecular H-transfer within 60 fs. The Stokes-shifted fluorescence was explained by tautomerization involving distortion of the entire molecular skeleton rather than formation of a zwitterionic species via a fast localized proton-transfer process.

This wealth of information available for ESIPT of MS and related compounds is contrasted by the lack of similar data on their naphthalene analogues, methyl 1-hydroxy-2-naphthoate (1H2MN), 1-hydroxy-2-acetonaphthone (1H2AN), and 1-hydroxy-2-naphthaldehyde (1H2NA) (see Chart 1). Recently, Douhal and co-workers[40] have studied the dynamic behavior of excited 1H2AN in a supersonic molecular beam. In the dispersed fluorescence spectra, they observed a dual fluorescence in two close but different spectral regions. The blue fluorescence with a resolved vibrational pattern was assigned to the parent enol form, and the second broad one with peaks at 426 and 451 nm was attributed to the tautomeric keto-form. Catalán and del Valle[41] have reported that 1H2AN was significantly more photostable than a well-known photostabilizer, 2-(2′-hydroxy-5′-methylphenyl)benzotriazole (Tinuvin P) in dimethyl sulfoxide. However, they have concluded that a usual ESIPT process was not included in 1H2AN and the photostability was not attributable to the formation of a complete keto-form. Therefore, photophysical properties of 1H2AN are of interest, and more detailed studies including comparisons with those of related compounds (1H2NA and 1H2MN) are required.

CHART 1

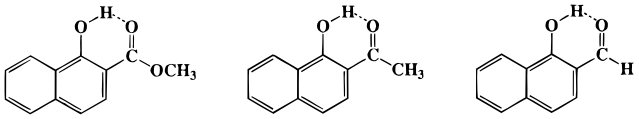

The aim of the present study is to clarify the following aspects: (1) whether ESIPT occurs in 1H2MN, 1H2AN, and 1H2NA or not, (2) dynamics of reverse proton-transfer reaction in the ground state including solvent perturbations, and (3) effects of substituent in the carbonyl group on the electronic structure and photophysical properties of intramolecularly hydrogen bonded 1H2MN, 1H2AN, and 1H2NA.

2. Experimental Section

2.1. Materials. 1-Hydroxy-2-acetonaphthone (1H2AN; Aldrich) and 1-hydroxy-2-naphthaldehyde (1H2NA; Tokyo Kasei) were purified by recrystallization followed by vacuum sublima-

S1089-5639(98)01368-1 CCC: $15.00
Published on Web 06/05/1998

tion. Methyl 1-hydroxy-2-naphthoate (1H2MN) was synthesized by esterification of 1-hydroxy-2-naphthoic acid (Aldrich). The product was purified by column chromatography followed by recrystallization and was identified by mass spectrometry and NMR. Cyclohexane (Kishida) was purified by column chromatography, dried over metallic sodium, and fractionally distilled. 3-Methylpentane (Wako, special grade) and methylcyclohexane (Aldrich, spectrophotometric grade) were dried over molecular sieves 4A, refluxed for several hours over lithium aluminum hydride under nitrogen atmosphere, and fractionally distilled prior to use. Acetonitrile (Kishida, spectrosol) was dried over molecular sieves 4A and distilled from P_2O_5. Traces of P_2O_5 were then removed by distillation from anhydrous K_2CO_3. 1-Propanol (Wako, special grade) was distilled from anhydrous K_2CO_3. Dimethyl sulfoxide (Wako, UV spectral grade) was distilled under reduced pressure. Methanol (Wako) and ethanol (Wako) were purified by fractional distillation. 2,2,2-Trifluoroethanol (Wako, special grade) and ethanol-d_1 (Aldrich, 99.5%) were used as received. Triethylamine (Wako, special grade) was purified by distillation under reduced pressure.

2.2. Methods. Absorption and fluorescence spectra were recorded on a Jasco Ubest-50 spectrophotometer and a Hitachi F-4010 spectrofluorometer with a rhodamine B quantum counter for spectral correction, respectively. The fluorescence quantum yield (Φ_f) was determined by using a 1 N H_2SO_4 solution of quinine bisulfate ($\Phi_f = 0.546$) as standard.[42] Fluorescence lifetime was obtained with a time-correlated single-photon-counting fluorometer (Edinburgh Analytical Instruments, FL900CDT). For the determination of lifetimes less than 1 ns, a picosecond laser system consisting of a Nd^{3+}:YAG laser (Continuum PY 61-10; 355 nm; fwhm, ~40 ps) and a streak scope (Hamamatsu C4334) was used. Infrared absorption spectra were measured with a FT-IR spectrophotometer (Perkin Elmer model 1600). NMR spectra were recorded on a JEOL Alpha-500 FT NMR spectrometer. Chemical shifts (δ) in ppm were measured in $CDCl_3$ referred to tetramethylsilane (TMS) as internal standard.

Transient absorption spectra were measured by using a nanosecond laser photolysis system consisting of a Nd^{3+}:YAG laser (Spectra Physics, GCR-130, pulse width 5 ns) as an excitation source and a 150 W xenon flash lamp (Ushio UXL151D) as monitoring light. For the decay measurements of transients with lifetime above 50 μs, the pulsed xenon lamp system was replaced by a low-drift and low-fluctuation lamp system consisting of a 150 W short-gap xenon lamp (Hamamatsu, L2274) and a high-voltage electric source (Hamamatsu C4263). The transient signals were recorded on a digitizing oscilloscope (Tektronix, TDS-744; 500 MHz 2 G samples) and transferred to a personal computer (NEC, PC-9821Ap).

Details for the apparatus of the time-resolved thermal lensing (TRTL) measurements were reported elsewhere.[43] Briefly, the third harmonic (355 nm) of a Nd^{3+}:YAG laser (Spectra Physics GCR-130, pulse width 5 ns) or the 308 nm pulse of a XeCl excimer laser (Lambda Physik, Lextra 50, pulse width 17 ns) was used as an excitation source. A He−Ne laser (NEC, GLG2026; 633 nm) focused coaxially with the excitation beam was used as a probe beam for the TRTL signals. The signals were detected by a photomultiplier tube (Hamamatsu, R928) after passing through a monochromator (JOBIN-YVON, H-20). The absorbance of the sample solutions was adjusted to ~0.1 at 355 or 308 nm.

X-ray crystallographic measurements were made on a Rigaku AFC7S diffractometer with graphite monochromated Cu Kα radiation. The details for the X-ray crystallographic analysis were reported elsewhere.[44] Briefly, a colorless prismatic crystal with approximate dimensions of 0.40 × 0.20 × 0.20 mm was mounted on a glass fiber. Cell constants and an orientation matrix for data collection, obtained from a least-squares refinement using the setting angles of 25 carefully centered reflections in the range $40.8° < 2\theta < 49.3°$, corresponded to a primitive triclinic cell with dimensions $a = 9.052(1)$ Å, $b = 13.631(2)$ Å, $c = 8.729(2)$ Å, $\alpha = 108.34(2)°$, $\beta = 102.72(2)°$, $\gamma = 98.30(1)°$, $V = 970.2(4)$ Å^3. The space group was determined to be $P\bar{1}$(#2). The data were collected at a temperature of 20 ± 1 °C using the $\omega-2\theta$ scan technique to a maximum 2θ value of 120.1°.

Molecular orbital calculations were performed by use of the ab initio MO method (Gaussian 94)[45] on an IBM RS/6000 workstation (model 41T). The molecular geometries of 1H2AN and 1H2MN were optimized at the Hartree−Fock (HF)/3-21G level for the ground state, whereas in the optimizations for the excited-state geometries the configuration interaction scheme with single excitations (CIS) was used. The contraint of C_s symmetry was maintained throughout all optimizations.

TABLE 1: IR and NMR Data of 1H2MN, 1H2AN, and 1H2NA

compound	ν_{O-H} (cm^{-1})	$\Delta\nu_{O-H}$ (cm^{-1})	$\nu_{C=O}$ (cm^{-1})	$\Delta\nu_{C=O}$ (cm^{-1})	δ_{O-H} (ppm)	$\Delta\delta_{O-H}$ (ppm)
1H2MN	3067	−549[a]	1670	−56[b]	11.98	6.57[e]
1H2AN	2722	−894[a]	1628	−57[c]	14.01	8.60[e]
1H2NA	2940	−676[a]	1650	−52[d]	12.67	7.26[e]

[a] The displacement of the OH band from the position (3616 cm^{-1}) in 1-naphthol.[46] [b] The displacement of the CO band from the position (1726 cm^{-1}) in 2-methylnaphthoate.[47] [c] The displacement of the CO band from the position (1685 cm^{-1}) in 2-acetonaphthone.[47] [d] The displacement of the CO band from the position (1702 cm^{-1}) in 2-naphthaldehyde.[47] [e] The displacement of the OH chemical shift from that ($\delta_{O-H} = 5.41$) in 1-naphthol.[48]

3. Results and Discussion

3.1. Intramolecular Hydrogen Bond in the Ground State. In order to evaluate the strength of intramolecular hydrogen bonds in 1H2MN, 1H2AN, and 1H2NA, the IR and NMR spectra were measured. Table 1 shows the characteristic IR frequencies (O−H and C═O stretchings) of 1H2MN, 1H2AN, and 1H2NA in CCl_4 and the OH chemical shifts of their proton NMR spectra in $CDCl_3$ at room temperature. The O−H stretching bands (ν_{OH}) are found to appear at considerably lower frequencies compared with those of 1-naphthol, and also significant decreases in the C═O stretching frequencies ($\nu_{C=O}$) of 1H2MN, 1H2AN, and 1H2NA can be seen relative to those of methyl 2-naphthoate, 2-acetonaphthone, and 2-naphthaldehyde. The C═O stretching frequencies shown in Table 1 are in good agreement with the reported values.[46,47] On the other hand, the chemical shifts of the hydroxyl group in the NMR spectra show remarkable increases for 1H2AN, 1H2NA, and 1H2MN compared with that of 1-naphthol. Since solute concentration effects are negligible for both IR and NMR spectra, these drastic changes in the IR and NMR spectra can be ascribed to strong intramolecular hydrogen bonds in these compounds. According to Zadorozhnyi and Ishchenko,[46,49] the hydrogen-bond energy (E_{hb}) can be expressed by the relation $\Delta\nu_{C=O}/\nu_{C=O} = -K_{C=O}E_{hb}$, where $\Delta\nu_{C=O}$ and $K_{C=O}$ are the magnitude of the spectral shift and proportionality coefficient reported to be 9.6×10^{-4} mol kJ^{-1}.[46] According to the above relation, it can be estimated that the strengths of the intramolecular hydrogen bond of 1H2MN, 1H2AN, and 1H2NA in the

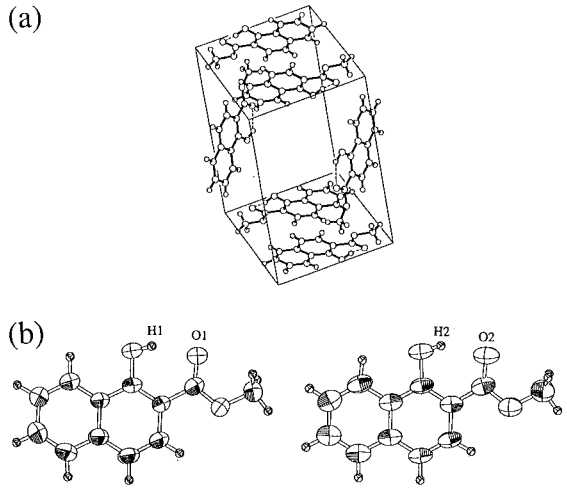

Figure 1. (a) Packing of the molecules and (b) solid-state conformations of 1H2MN.

ground state are 35, 36, and 33 kJ mol^{-1}. In addition to the formation of strong intramolecular hydrogen bonds, the presence of the hydrogen atom at the peri-position of the naphthalene ring would hinder development of the open form (hydrogen-bond broken form) even in highly polar solvents, as pointed out by Catalán and del Valle.[41]

As in the case of MS, 1H2MN possesses two distinct sites (carbonyl and ester oxygen atoms) which can form an intramolecular hydrogen bond. Two distinct fluorescence bands (ultraviolet and blue) observed upon photoexcitation of MS have been attributed to the ground-state rotamer which have an intramolecular hydrogen bond between hydroxy proton and ester or carbonyl oxygen atoms.[23−30,50] Similarly 1H2MN has a possibility to form two different rotamers. Therefore, X-ray crystallographic analyses were performed for 1H2MN to elucidate the predominant molecular structures in the ground state. Figure 1 shows the packing of the molecules and two slightly different molecular structures in the unit cell obtained by X-ray crystallographic analyses of a 1H2MN crystal. The results of the X-ray crystallographic analyses clearly indicate that the structure of 1H2MN in the ground state has an intramolecular hydrogen bond between the OH and C═O groups. The distances associated with the hydrogen bonds H1−O1 and H2−O2 are 1.835 and 1.875 Å, respectively. These distances are longer than the hydrogen-bond distance (1.704 Å) reported for salicylic acid.[51]

It can be concluded that the three compounds investigated in the present study have the same type of intramolecular hydrogen bonds, although the strength is modified depending upon substituents. Nevertheless, very different photophysical properties were found for these three compounds, as described below.

3.2. Photophysical Properties. The absorption and fluorescence spectra of 1H2MN, 1H2AN, and 1H2NA in cyclohexane at room temperature are shown in Figure 2 together with their fluorescence excitation spectra. The fluorescence excitation spectrum coincides well with the corresponding absorption spectrum for all the compounds. The molar extinction coefficients of the first absorption maximum of 1H2MN, 1H2AN, and 1H2NA are 5100 M^{-1} cm^{-1} (at 342 nm), 7800 M^{-1} cm^{-1} (at 365 nm), and 5690 M^{-1} cm^{-1} (at 368 nm), respectively, showing a character of (π,π*) transitions for the first absorption band. It is noteworthy here that 1H2AN and 1H2NA show similar spectral properties; however, that of 1H2MN is markedly different from the former two compounds. The Stokes shift for 1H2MN (3390 cm^{-1}) is much smaller than those (6120 and

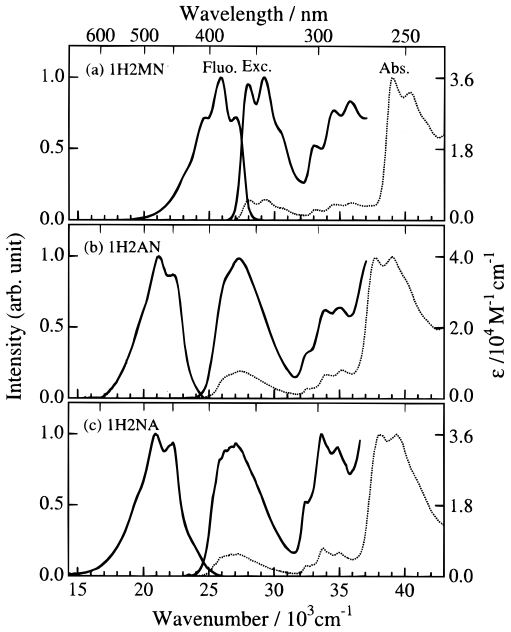

Figure 2. Absorption (dotted line), fluorescence, and fluorescence excitation (solid line) spectra of (a) 1H2MN (λ_{ex} = 342 nm, λ_{em} = 386 nm), (b) 1H2AN (λ_{ex} = 365 nm, λ_{em} = 470 nm), and (c) 1H2NA (λ_{ex} = 368 nm, λ_{em} = 476 nm) in cyclohexane at 293 K.

TABLE 2: Fluorescence Lifetime (τ_f), and Quantum Yields for Fluorescence (Φ_f), Intersystem Crossing (Φ_{isc}) and Internal Conversion (Φ_{ic}) of 1H2MN, 1H2AN, and 1H2NA in Cyclohexane at 293 K and in 3-Methylpentane at 77 K

	T: 293 K				T: 77 K	
compound	τ_f (ns)	Φ_f	Φ_{isc}	Φ_{ic}	τ_f (ns)	Φ_f
1H2MN	2.39	0.42	0.35	0.23	4.59	0.55
1H2AN	0.045	0.005			7.80	0.23
1H2NA	0.85	0.023			8.29	0.19

6170 cm^{-1}) of 1H2AN and 1H2NA. In benzene analogues of these compounds (MS, OHAP, and OHBA), much larger Stokes shifts (ca. 10 000 cm^{-1}) have been reported for the emission from the proton-transferred form.

From the relatively small Stokes shifts and also the fact that the absorption and fluorescence spectra were almost mirror-images of each other, Catalán and del Valle[41] have considered that ESIPT was not involved in 1H2AN. On the other hand, Douhal et al.[40] have reported that the emission from the vibrationless level of the S_1 state of 1H2AN isolated in a supersonic expansion exhibited a dual character. The short-wavelength fluorescence (∼1400 cm^{-1} from the origin) was highly structured, and its vibrational structure correlated with that of the S_1 state. The long-wavelength part shifted by ∼2200 and 3500 cm^{-1} was more intense and diffuse. These results were interpreted in terms of excited-state intramolecular proton (or hydrogen atom) transfer from the initial enol-form to the tautomeric keto-conformer through a small energy barrier between two closely lying local potential minima.

We examined photophysical properties of 1H2AN and related compounds in cyclohexane at 293 K and in 3-methylpentane at 77 K. Photophysical parameters obtained are summarized in Table 2. For the determination of the quantum yield of intersystem crossing (Φ_{isc}), the TRTL method[52−54] was employed. The TRTL signals obtained by 355 nm excitation of 1H2MN, 1H2AN, and 1H2NA in cyclohexane at 293 K are shown in Figure 3. A clear difference is seen in their time profiles; the TRTL signal of 1H2MN shows fast and slow rise components, in which the latter corresponds to slow thermal

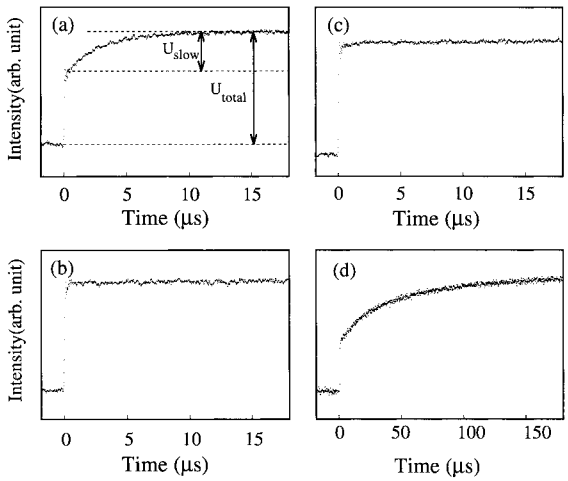

Figure 3. Time evolution of the TRTL signals of (a) 1H2MN, (b) 1H2AN, (c) 1H2NA ($\lambda_{exc} = 355$ nm), and (d) 1-methoxy-2-acetonaphthone ($\lambda_{exc} = 308$ nm) in cyclohexane at 293 K.

release from the lowest triple state. In contrast, the time profiles of 1H2AN and 1H2NA consist almost exclusively of a prompt rise component. Figure 3 also includes the TRTL signal of 1-methoxy-2-acetonaphthone in which effects of intramolecular hydrogen bond are not observable. This compound shows a substantial slow rise component, demonstrating that the triplet state is efficiently formed. These observations indicate that in 1H2AN and 1H2NA there exist fast nonradiative deactivation processes with rate constants much larger than that of intersystem crossing in the parent S_1 state. ESIPT and/or internal conversion are anticipated to be possible candidates for such an efficient nonradiative process.

For 1H2MN, it can be assumed that ESIPT does not occur as shown below; therefore, the Φ_{isc} value can be determined according to the following relation by measurements of the ratio of the slow and total TRTL signal intensities (U_{slow}/U_{total}):

$$\frac{U_{slow}}{U_{total}} = \frac{\Phi_{isc} E_T}{E_{ex} - \Phi_f \langle E_S \rangle} \tag{1}$$

where E_{ex} and E_T are the excitation energy and 0−0 transition energy of the lowest triplet state, respectively, and $\langle E_S \rangle$ is the average energy dissipated by fluorescence from the S_1 state. $\langle E_S \rangle$ is given by

$$\langle E_S \rangle = \frac{\int \bar{\nu} I_f(\bar{\nu})\, d\bar{\nu}}{\int I_f(\bar{\nu})\, d\bar{\nu}} \tag{2}$$

where $I_f(\bar{\nu})$ is the spectral distribution of fluorescence in wavenumber ($\bar{\nu}$). The calculated value of $\langle E_S \rangle$ for 1H2MN was 25 280 cm^{-1}. The E_T value for 1H2MN was estimated from its phosphorescence spectrum in 3-methylpentane at 77 K to be 20 860 cm^{-1}. To apply eq 1 for the determination of Φ_{isc}, one has to use the monitoring wavelength for the TRTL signals where the contribution from $T_n \leftarrow T_1$ absorption is negligible. It was confirmed that at 633 nm this condition adequately held in 1H2MN (see Figure 4). By assuming the relation $\Phi_{ic} = 1 - \Phi_f - \Phi_{isc}$, the values of Φ_{isc} and Φ_{ic} were determined as shown in Table 2. The rate constants of fluorescence (k_f), intersystem crossing (k_{isc}), and internal conversion (k_{ic}) for 1H2MN were calculated from the quantum yields and the fluorescence lifetime as 1.8×10^8, 1.5×10^8, and 0.9×10^8 s^{-1}, respectively. The photophysical parameters obtained for 1H2MN show relaxation properties of usual excited organic molecules.

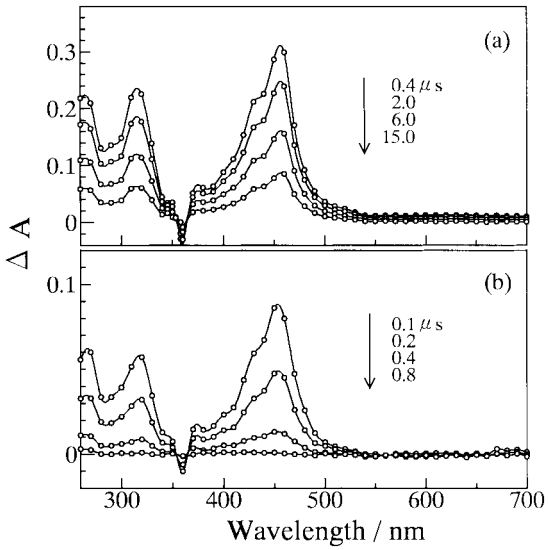

Figure 4. Transient absorption spectra obtained by 355 nm laser photolysis of 1H2MN in (a) degassed and (b) aerated cyclohexane at 293 K.

On the other hand, photophysical properties of 1H2AN and 1H2NA are totally distinct from that of 1H2MN. The fluorescence lifetimes of 1H2AN and 1H2NA at 293 K are much smaller that that of 1H2MN, and the total quantum yield for nonradiative processes from the parent S_1 state is close to unity. These observations indicate that rapid radiationless processes from the fluorescent state are involved for 1H2AN and 1H2NA. The fluorescence lifetime and quantum yield of 1H2AN and 1H2NA increase greatly with a decrease in temperature, indicating the presence of temperature-dependent nonradiative processes. Such a feature has been commonly observed for the fluorescence from the proton-transferred form in the excited state.[24,35,55,56] Thus, it is conceivable from the photophysical properties and the relatively large Stokes shift that 1H2AN and 1H2NA undergo ESIPT in solution.

3.3. Transient Absorption Spectra. The occurrence of ESIPT in 1H2AN and 1H2NA and its absence in 1H2MN are supported by observation of transient absorption due to the proton-transferred tautomer in the ground state. Figure 4 shows the transient absorption spectra obtained by 355 nm laser photolysis of 1H2MN in cyclohexane at room temperature for both degassed and aerated solutions. The degassed sample (Figure 4a) shows a transient with absorption maxima at 265, 315, and 455 nm. The decay kinetics of these absorption bands follow the same mixed first- and second-order kinetics. Under aerated conditions (Figure 4b), a remarkable quenching by dissolved oxygen can be seen. From these facts the transient obtained by 355 nm laser photolysis of 1H2MN can be assigned to the triplet state. The observation of such strong $T_n \leftarrow T_1$ absorption bands for 1H2MN is consistent with the relatively large Φ_{isc} value (0.35) determined by TRTL measurements. No other transients are recognized for both absorption spectra in Figure 4.

On the other hand, the transient absorption spectra obtained for 1H2AN are significantly different from those of 1H2MN, as shown in Figure 5. The main absorption bands are seen at 275 and 400 nm. The decay rates of these absorption bands are not affected by the presence of oxygen, as can be seen from Figure 5a,b. Thus, the transient giving the absorption maxima

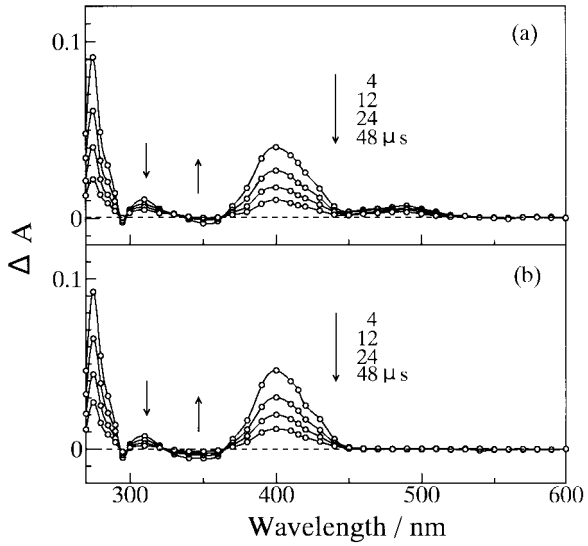

Figure 5. Transient absorption spectra obtained by 355 nm laser photolysis of 1H2AN in (a) degassed and (b) aerated cyclohexane solutions at 293 K.

at 275 and 400 nm can be ascribed to a ground-state transient produced by 355 nm laser photolysis of 1H2AN. A possibility of a 1H2AN anion produced by proton ejection in the excited state or in the ground-state tautomer can be excluded by the following experimental facts: (1) the transient absorption spectrum taken for 1H2AN in ethanol was not identical with the differential absorption spectrum obtained by subtracting the steady-state absorption spectrum of 1H2AN in EtOH from that of the 1H2AN anion in a 10^{-2} M KOH/EtOH solution; (2) the long-lived transient was observed clearly even in dried hydrocarbon solvents. In the degassed solution (Figure 5a), another weak absorption band is seen at around 490 nm. Since this band is quenched almost completely by dissolved oxygen, it can be ascribed to the $T_n \leftarrow T_1$ absorption of 1H2AN. This assignment was confirmed by triplet sensitization experiments using naphthalene in cyclohexane as a triplet sensitizer. The transient absorption spectra of 1H2NA were similar to those of 1H2AN in spectral shape and kinetic behavior, although the absorption intensity measured under the same experimental condition was smaller than that of 1H2AN.

Figure 6 shows the transient absorption spectra taken at 0.5−6.0 μs after 355 nm laser photolysis of 1H2AN in methanol (MeOH). With a lapse in time the absorption peak at 420 nm is shifted to shorter wavelengths, and the absorption spectra at the delay times longer than ~6.0 μs almost coincide with the differential absorption spectrum (Figure 6b; solid line) generated by subtracting the steady-state absorption spectrum of 1H2AN in MeOH from that of the 1H2AN anion in a 10^{-2} M KOH/MeOH solution. The time trace monitored at 400 nm consists of two exponential components with rate constants of 8.7×10^5 and 3.1×10^4 s^{-1}, as shown in the inset of Figure 6. The long-lifetime component at ~400 nm was significantly quenched by adding a small amount of acetic acid in the solution. These observations indicate that the 1H2AN anion is produced by excitation of 1H2AN in polar methanol. One possible mechanism to produce the 1H2AN anion may be excited-state proton ejection to solvent. Another plausible route is the formation of the ground-state keto-tautomer through ESIPT followed by proton transfer to solvent molecules. It is, however, difficult to distinguish between these two possibilities from the data in Figure 6 because of the spectral overlap between the 1H2AN anion and keto-tautomer. Similar anion formation has also been reported for other intramolecular hydrogen-bonded systems in

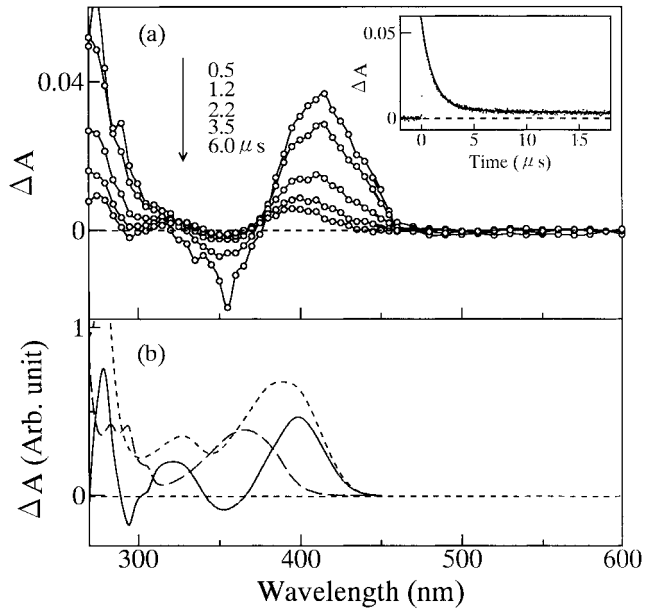

Figure 6. (a) Transient absorption spectra obtained by 355 nm laser photolysis of 1H2AN in methanol and the decay profile monitored at 400 nm (inset). (b) Steady-state absorption spectra of 1H2AN (− −) and 1H2AN anion (- - -) in methanol and their differential absorption spectrum (—) at 293 K.

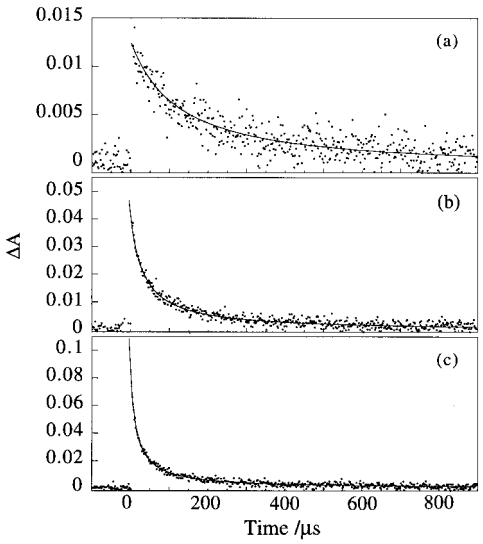

Figure 7. Time traces (monitored at 400 nm) of the transient absorption spectrum of 1H2AN in cyclohexane at 293 K at different laser intensities: (a) 2 mJ pulse^{-1} cm^{-2}, (b) 8 mJ pulse^{-1} cm^{-2}, and (c) 16 mJ pulse^{-1} cm^{-2}.

polar solvent.[37] For 3-hydroxyflavone it has been reported that the solute anion is produced even in hydrocarbon solvents when traces of water are present.[57] This is probably due to the relatively weak intramolecular hydrogen bond in 3-hydroxyflavone.

Judging from the photophysical properties and the result of transient absorption measurements, the long-lived transient obtained by 355 nm laser photolysis of 1H2AN is attributable to the tautomeric keto-form in the ground state.

3.4. Kinetic Behavior of the Ground-State Keto-Form Produced by 355 nm Laser Photolysis of 1H2AN. Kinetic behavior of the tautomeric keto-form was strongly affected by solvent environment. Figure 7 shows the time profiles of the transient absorption monitored at 400 nm under different laser intensities for 1H2AN in cycloohexane at 293 K. The time

TABLE 3: Decay Rate Constants of the Transient Absorption of 1H2AN in Various Solvents at 293 K (λ_{mon}: 400 nm)

solvent	k_1 (10^3 s^{-1})	k^{ROH} (10^5 s^{-1})	k_2 ($\epsilon \times 10^5$ M^{-1} s^{-1})
cyclohexane	2.1		9.8
methylcyclohexane	1.9		8.1
3-methylpentane	9.9		9.7
acetonitrile	0.32		
dimethyl sulfoxide	4.7		
ethanol		8.0	
methanol		8.9[a]	
1-propanol		7.7	
2,2,2-trifluoroethanol		0.22	
polystyrene film	5.04×10^{-3}		

[a] λ_{mon}: 440 nm.

profiles follow mixed first- and second-order decay kinetics. The contribution of the second-order component is found to increase with increasing laser intensities. Therefore, the decay kinetics of the keto-form (1H2AN′) at 400 nm in cyclohexane can be written as

$$-\frac{d[1H2AN']}{dt} = \{k_1 + k_2[1H2AN']\}[1H2AN'] \quad (3)$$

where k_1 and k_2 denote the first- and second-order decay rate constants. By least-squares fitting procedures, the best-fitted rate constants k_1 and k_2 in cyclohexane at 293 K, were obtained as 2.1×10^3 s^{-1} and $9.8\epsilon \times 10^5$ M^{-1} s^{-1}, respectively, where ϵ is the molar extinction coefficient of the transient at 400 nm. The decay properties of the 400 nm transient obtained by 355 nm laser photolysis of 1H2AN in various solvents are summarized in Table 3. The bimolecular decay process in addition to the first-order component is seen only in nonpolar hydrocarbon solvents, cyclohexane, methylcyclohexane, and 3-methylpentane. The bimolecular process is probably due to mutual hydrogen exchange through intermolecular hydrogen-bonding interactions between two tautomer molecules. In polar aprotic solvents, acetonitrile and dimethyl sulfoxide, only the unimolecular decay process with rate constants of 3.2×10^2 and 4.7×10^3 s^{-1}, respectively is seen.

Interestingly, the decay rate increases more than 2 orders of magnitude on going from nonpolar hydrocarbon to protic solvents. The effects of ethanol and deuterated ethanol on the decay rate of the transient were examined by measuring the decay rate at 400 nm as a function of the ethanol (or deuterated ethanol) concentration in cyclohexane at 293 K. In Figure 8a, logarithmic plots of the observed decay rate (k_{obs}) of 1H2AN′ versus log[EtOH] or log[EtOD] are shown. The k_{obs} of 1H2AN′ begin to increase from a concentration of approximately 2.5×10^{-3} M. The significant increase in k_{obs} indicates that there exists an alcohol molecule catalyzed decay process. The decay rate of 1H2AN′ in cyclohexane in the presence of ethanol can be written as

$$-\frac{d[1H2AN']}{dt} = \{k^{CH} + k^{EtOH}[EtOH]^n\}[1H2AN'] = k_{obs}[1H2AN'] \quad (4)$$

As $k^{CH} \ll k^{EtOH}[EtOH]^n$, the following relation is obtained.

$$\log k_{obs} = \log k^{EtOH} + n \log[EtOH] \quad (5)$$

The log−log plot in Figure 8a shows slopes of 3.0 and 2.7 for

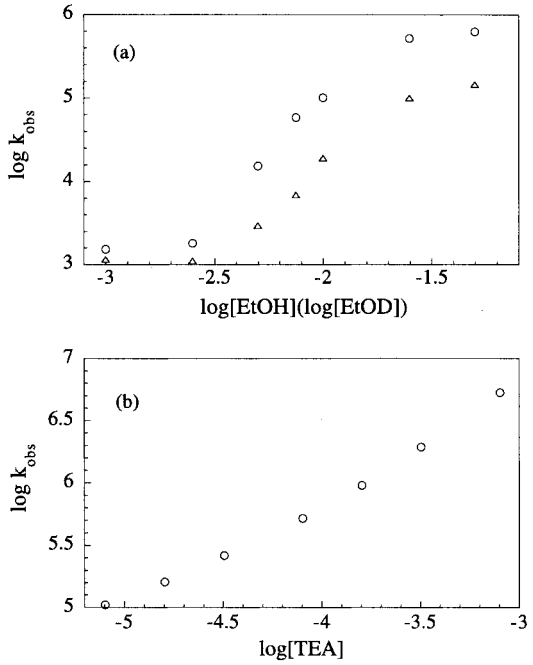

Figure 8. Effects of (a) ethanol (○) or ethanol-d_1 (△) in cyclohexane and (b) triethylamine (○) in methylcyclohexane on the observed decay rate (k_{obs}) at 400 nm of the transient obtained by 355 nm laser photolysis of 1H2AN at 293 K.

EtOH and EtOD in the concentration range $\sim 10^{-2.5}$ to $\sim 10^{-2.0}$ M. Therefore, more than two ethanol molecules are considered to participate in the ethanol-catalyzed decay processes in this concentration range. Figure 8a shows a relatively large isotope effect ($k_{obs}^{EtOH}/k_{obs}^{EtOD} = 5.3$ at a concentration of 10^{-2} M), indicating that the mutual proton transfer between 1H2AN′ and ethanol molecules plays an important role in the catalytic action.

The presence of inflection points in Figure 8a suggests that the decay processes of 1H2AN′ are also catalyzed by traces of water contained in cyclohexane. The concentration of moisture in cyclohexane was estimated to be $\sim 10^{-4}$ M by the Karl Fisher method under the present experimental conditions. Hence, the effects of water on the decay of 1H2AN′, which corresponds to k_1, cannot be excluded in our experiments.

Figure 8b shows the effect of triethylamine on the decay rate of 1H2AN′ in methylcyclohexane. The significant increase in k_{obs} with adding triethylamine is seen as in the case of ethanol, although the catalytic effect of triethylamine seems to be much larger than that of ethanol. This result and the fact that 2,2,2-trifluoroethanol has a smaller catalytic effect compared with that of ethanol suggest that the recovery process of the keto-tautomer to the parent enol-form is catalyzed more efficiently by basic triethylamine molecules.

The observed effects of additives on the decay rate of 1H2AN′ are analogous to solvent perturbations on proton-transfer reactions reported by Kasha.[58] We have also reported similar catalytic effects of alcohols and triethylamine on the rate of sigmatropic hydrogen shifts in the photorearranged intermediate of phenyl acetate[59] and *N*-acetylpyrrole.[60] Therefore, it can be concluded that mutual proton or hydrogen atom transfer between solute and solvent molecules catalyzes the recovery process of 1H2AN′ into parent enol 1H2AN.

If the structure of the keto-tautomer (1H2AN′) is a cis-keto-form ($^1K_{cis}$) as shown in Scheme 1, the reverse intramolecular proton-transfer rate (k_{-PT}) in the ground state is expected to be much faster than the observed decay rates ($k_{obs} = k_1 + k_2[1H2AN']$ or k^{ROH}) shown in Table 3, because the energetic

SCHEME 1: Energy Level Diagram of the Lowest Excited Singlet States of the Normal Form of 1H2AN and Its Tautomer Forms[a]

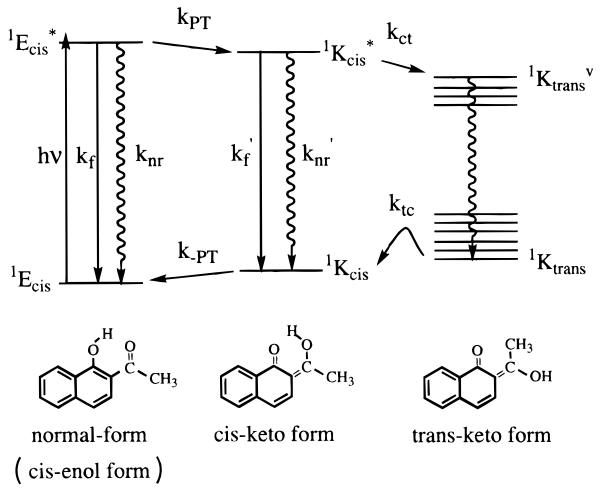

[a] The rate constant (k_{PT}) of the ESIPT process is considered to be much larger than k_f and k_{nr}; therefore, the observed fluorescence is ascribed to the fluorescence from the S_1 state of the cis-keto-form.

barrier would be small. In fact, Catalán et al. have recently obtained a single minimum for the ground-state reverse proton-transfer process of 1H2AN by using MP2 and B3LYP methods.[61] The above consideration and the significant decrease in the decay rate of 1H2AN′ (k_1) in polystyrene (see Table 3) suggest that the ESIPT process is followed by a structural change to produce a metastable state which can be detected by the nanosecond laser photolysis method. A plausible mechanism for the structural change is cis−trans isomerization [$^1K_{cis}$* → ($^1K_{trans}{}^V$) → $^1K_{trans}$] just after ESIPT (k_{PT}) as shown in Scheme 1. Here, $^1K_{trans}{}^V$ denotes higher vibrational states of $^1K_{trans}$. A similar cis−trans isomerization has been reported for *o*-hydroxyphenylbenzazoles.[62] In Scheme 1 the intrinsic isomerization rate (k_{tc}) of $^1K_{trans}$ to $^1K_{cis}$ in the ground state is expected to be much smaller than the k_1 value in Table 3, because k_1 is likely to include the perturbations due to traces of water in solvent. A rotational isomerization of the OH group following ESIPT is another candidate, as has been reported for OHAP and OHBA.[63] However, in 1H2AN the lifetime ($k_1{}^{-1}$) of the tautomer without bimolecular interactions is ∼1 ms in nonpolar aprotic solvent (see Table 3), which seems to be too slow in comparison with the formation rate of intramolecular hydrogen bond through internal rotation of the OH group.[64]

3.5. Electronic Structures and Photophysical Properties. As described above, the photophysical properties of 1H2MN are completely different from those of 1H2AN and 1H2NA, and it can be concluded that ESIPT does not occur in excited 1H2MN. It is, therefore, interesting to clarify the differences

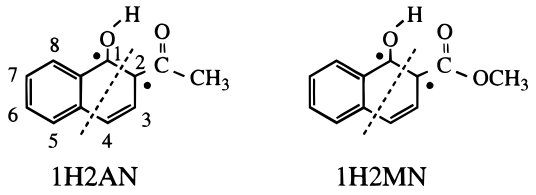

Figure 9. (a) Nodal plane character of the $S_1(^1L_a)$ state of 1H2AN and 1H2MN.

in the photophysical behaviors among three 1-naphthol derivatives from the viewpoint of the electronic character in the S_1 states.

First we consider the electronic properties of simplified analogues, methyl 2-naphthoate (2MN), 2-acetonaphthone (2AN), and 2-naphthaldehyde (2NA). The properties of the excited singlet and triplet states of all these compounds are known to depend strongly on solute-solvent interactions.[65,66] When 2AN or 2NA is dissolved in an alkane, the S_1 state is an (n,π*) state, and no fluorescence is observed. However, in alcohols or water 2AN and 2NA exhibit strong fluorescence, because the energy of the $S_2(\pi,\pi^*)$ state is lowered by hydrogen bonding than that of the lowest $^1(n,\pi^*)$ state. On the other hand, 2MN is strongly fluorescent even in an alkane solvent, because the energy level of the $^1(n,\pi^*)$ state is raised by an electron-donating substituent (−OCH_3) and the $^1(\pi,\pi^*)$ state becomes the lowest excited singlet state. In the cases of 1H2MN, 1H2AN, and 1H2NA, the intramolecular hydrogen-bonding interactions are included, so that the situation is somewhat complicated in comparison with the intermolecular hydrogen-bonding interactions between solute and solvent molecules. However, the tendency such that hydrogen-bonding interactions raise the $^1(n,\pi^*)$ level against the $^1(\pi,\pi^*)$ level can be assumed to be similar both in inter- and intramolecular interactions. Therefore, the S_1 state of 1H2MN is considered to have $^1(\pi,\pi^*)$ character, while for the S_1 state of 1H2AN and 1H2NA, $^1(n,\pi^*)$ and $^1(\pi,\pi^*)$ levels are anticipated to lie in close proximity.

Until recently, a large number of studies on ESIPT have been reported. In almost all the proton-transfer systems, the proton transfer is considered to take place from the $^1(\pi,\pi^*)$ state of parent molecules. Recent MO theoretical studies by Sobolewski and Domcke[21] on OHBA showed that the $^1(\pi,\pi^*)$ potential energy function was found to be barrierless along the proton-transfer reaction coordinate, while the $^1(n,\pi^*)$ potential energy exhibited a significant barrier. Therefore, it would be reasonable to assume that the ESIPT in 1H2AN and 1H2NA occurs in the $^1(\pi,\pi^*)$ state, although proximity effects[67] between the closely lying $^1(\pi,\pi^*)$ and $^1(n,\pi^*)$ states have influence to some extent on the ESIPT dynamics.

Recently, Nagaoka and Nagashima have developed a new description of the occurrence of ESIPT by considering the nodal pattern of the wave function and the delocalization of the π lone electrons in the excited state.[17−19,68] According to the

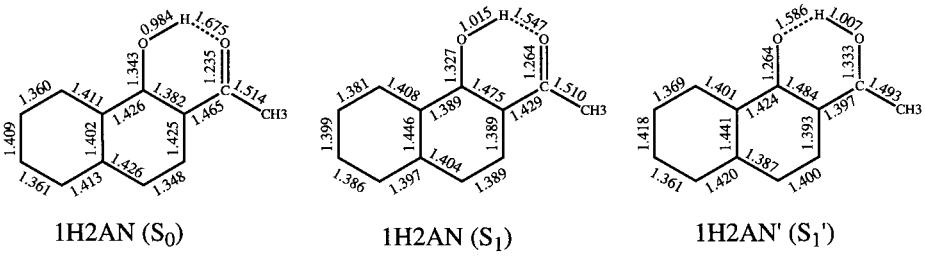

Figure 10. Optimized geometries (in Å) of the parent S_0, $S_1(\pi,\pi^*)$, and keto-tautomer $S_1'(\pi,\pi^*)$ states of 1H2AN. The optimizations were carried out by HF/3-21G and CIS/3-21G calculations.

"nodal plane" model, a nodal plane passes between the two oxygen atoms in the S_1 (^1L_a) state of 1H2AN and 1H2MN, as shown in Figure 9. Here two unpaired electrons are localized in the C_1 and C_2 carbon atoms and facilitate the rearrangement of bonds to produce the enol-tautomer. Stability of the $S_1^{(\pi)}$ state is considered to depend on the substituent bonded to the carbonyl group.[17] In both 1H2AN and 1H2MN, the delocalization of the π lone electron on C_2 is depressed owing to the presence of the electron-donating substituent (CH_3 and OCH_3 groups). This depressing effect would be larger in 1H2MN because of the greater π-electron-donating property of the methoxy group compared with that of the methyl group.

In order to confirm the substituent effect considered above, ab initio MO calculations were performed for the excited singlet states of 1H2AN and 1H2MN. The optimized S_1 state ($^1E_{cis}$*) of 1H2AN became a (π,π*) state, and a S_2(n,π*) level was found to locate slightly higher (5.4 kJ mol^{-1}) in energy. The energy level of the optimized S_1' state ($^1K_{cis}$*) of the cis-keto-form was 9.8 kJmol^{-1} lower than that of the parent S_1 state, consistent with the occurrence of ESIPT in 1H2AN. In contrast, the tautomer S_1' level of 1H2MN was 21.2 kJ mol^{-1} higher in energy relative to that of the S_1 state, supporting the above consideration based on the "nodal plane" model. It can also be found that the change in bond distances upon photoexcitation of 1H2AN shown in Figure 10 substantiates the present experimental results. The hydrogen-bond distance (1.675 Å) of the S_0 state of 1H2AN is significantly shortened upon photoexcitation (1.547 Å in S_1), while the C_1-C_2 distance is elongated by ~0.1 Å in accord with the nodal plane character in the S_1 state. As a whole, the bond distances in the S_1 state of 1H2AN are found to become close to those of the keto-tautomer S_1' state.

4. Conclusions

A comparative study of photophysical and photochemical processes of intramolecularly hydrogen-bonded molecules, 1H2AN, 1H2NA, and 1H2MN, was carried out to clarify substituent effects on the relaxation properties. Remarkable substituent effects were found for the relaxation processes. The S_1 state of 1H2AN and 1H2NA showed intramolecular proton transfer followed by relaxations to produce a long-lived ground keto-tautomer. The decay rate of the keto-tautomer was significantly enhanced by additives such as alcohols and triethylamine through cooperative proton transfer in nonpolar solvent. On the other hand, there was no indication of ESIPT for 1H2MN. The substituent effects on the occurrence of ESIPT were reasonably explained on the basis of the "nodal plane" model by Nagaoka and Nagashima. The results of ab initio MO calculations showed the ESIPT reaction to be exothermic for 1H2AN but to be endothermic for 1H2MN, consistent with the experimental results obtained and also the prediction based on the "nodal plane" model.

Acknowledgment. The authors would like to thank Professor H. Takahashi of Waseda University, Professor S. Tero-Kubota of Tohoku University, and Professor S. Nagaoka of Ehime University for their helpful discussions. We also thank Professor S. Tajima of Gunma College of Technology for measurements of mass spectra. This work was supported by a Grant-in-Aid on Priority-Area-Research Photoreaction Dynamics (06239101) from the Ministry of Education, Science and Culture of Japan.

Supporting Information Available: Details of the results of X-ray crystallographic analyses on 1H2MN (14 pages). Ordering information is given on any current masthead page.

References and Notes

(1) Douhal, A.; Lahmani, F.; Zewail, A. H. *Chem. Phys.* **1996**, *207*, 477.
(2) Kasha, M.; Heldt, J.; Gormin, D. *J. Phys. Chem.* **1995**, *99*, 7281.
(3) Elsaesser, T. In *Femtosecond Chemistry*; Manz, J., Wöste, L., Eds.; VCH Verlag: Weinheim, 1994.
(4) Formosinho, S. J.; Arnaut, L. G. *J. Photochem. Photobiol. A* **1993**, *75*, 21.
(5) Barbara, P. F.; Walsh, P. K.; Brus, L. E. *J. Phys. Chem.* **1989**, *93*, 29.
(6) Kosower, E. M.; Huppert, D. *Annu. Rev. Phys. Chem.* **1986**, *37*, 127.
(7) Weller, A. *Z. Elektrochem.* **1956**, *60*, 1144.
(8) Lahmani, F.; Zehnacker-Rentien, A. *J. Phys. Chem. A* **1997**, *101*, 6141.
(9) Gormin, D.; Sytnik, A.; Kasha, M. *J. Phys. Chem. A* **1997**, *101*, 672.
(10) McGarry, P. F.; Jockusch, S.; Fujiwara, Y.; Kaprinidis, N. A.; Turro, N. J. *J. Phys. Chem. A* **1977**, *101*, 764.
(11) Guallar, V.; Moreno, M.; Lluch, J. M.; Amat-Guerri, F.; Douhal, A. *J. Phys. Chem.* **1996**, *100*, 19789.
(12) Keck, J.; Kramer, H. E. A.; Port, H.; Hirsch, T.; Fischer, P.; Rytz, G. *J. Phys. Chem.* **1996**, *100*, 14468.
(13) Parsapour, F.; Kelley, D. F. *J. Phys. Chem.* **1996**, *100*, 2791.
(14) Tarkka, R. M.; Jenekhe, S. A. *Chem. Phys. Lett.* **1996**, *260*, 533.
(15) Zhang, H.; van der Meulen, P.; Glasbeek, M. *Chem. Phys. Lett.* **1996**, *253*, 97.
(16) Mitra, S.; Das, R.; Bhattacharyya, S. P.; Mukherjee, S. *J. Phys. Chem. A* **1997**, *101*, 293.
(17) Nagaoka, S.; Shinde, Y.; Mukai, K.; Nagashima, U. *J. Phys. Chem. A* **1997**, *101*, 3061.
(18) Nagaoka, S.; Nagashima, U. *J. Phys. Chem.* **1990**, *94*, 1425.
(19) Nagaoka, S.; Nagashima, U. *Chem. Phys.* **1989**, *136*, 153.
(20) Verner, M. V.; Scheiner, S. *J. Phys. Chem.* **1995**, *99*, 642.
(21) Sobolewski, A. L.; Domcke, W. *Chem. Phys.* **1994**, *184*, 115.
(22) Catalán, J.; Palomar, J.; De Paz, J. L. G. *J. Phys. Chem. A* **1997**, *101*, 7914.
(23) Law, K-Y.; Shoham, J. *J. Phys. Chem.* **1995**, *99*, 12103.
(24) Law, K-Y.; Shoham, J. *J. Phys. Chem.* **1994** *98*, 3114.
(25) Herek, J. L.; Pedersen, S.; Bañares, L.; Zewail, A. H. *J. Chem. Phys.* **1992**, *97*, 9046.
(26) Orton, E.; Morgan, M. A.; Pimentel, G. C. *J. Phys. Chem.* **1990**, *94*, 7936.
(27) Acuña, A. U.; Toribio, F.; Amat-Guerri, F.; Catalán, J. *J. Photochem.* **1985**, *30*, 339.
(28) Toribio, F.; Catalán, J.; Amat, F.; Acuña, A. U. *J. Phys. Chem.* **1983**, *87*, 817.
(29) López-Delgado, R.; Lazare, S. *J. Phys. Chem.* **1981**, *85*, 763.
(30) Acuña, A. U.; Amat-Guerri, F.; Catalán, J.; González-Tablas, *J. Phys. Chem.* **1980**, *84*, 629.
(31) Smith, K. K.; Kaufmann, K. J. *J. Phys. Chem.* **1978**, *82*, 2286.
(32) Goodman, J.; Brus, L. E. *J. Am. Chem. Soc.* **1978**, **100**, 7472.
(33) Peteanu, L. A.; Mathies, R. A. *J. Phys. Chem.* **1992**, *96*, 6910.
(34) Nishiya, T.; Yamauchi, S.; Hirota, N.; Baba, M.; Hanazaki, I. *J. Phys. Chem.* **1986**, *90*, 5730.
(35) Nagaoka, S.; Hirota, N.; Sumitani, M.; Yoshihara, K. *J. Am. Chem. Soc.* **1983**, *105*, 4220.
(36) Morgan, M. A.; Orton, E.; Pimentel, G. C. *J. Phys. Chem.* **1990**, *94*, 7927.
(37) Nagaoka, S.; Nagashima, U.; Ohta, N.; Fujita, M.; Takemura, T. *J. Phys. Chem.* **1988**, *92*, 166.
(38) Nagaoka, S.; Hirota, N.; Sumitani, M.; Yoshihara, K.; Lipczynska-Kochany, E.; Iwamura, H. *J. Am. Chem. Soc.* **1984**, *106*, 6913.
(39) Catalán, J.; Toribio, F.; Acuña, A. U. *J. Phys. Chem.* **1982** *86*, 303.
(40) Douhal, A.; Lahmani, F.; Zehnacker-Rentien, A. *Chem. Phys.* **1993**, *178*, 493.
(41) Catalán, J.; del Valle, J. C. *J. Am. Chem. Soc.* **1993**, *115*, 4321.
(42) Eaton, D. F. *Pure Appl. Chem.* **1988**, *60*, 1107.
(43) Suzuki, K.; Tanabe, H.; Tobita, S.; Shizuka, H. *J. Phys. Chem. A* **1997**, *101*, 4496.
(44) Nakamura, Y.; Tsuihiji, T.; Mita, T.; Minowa, T.; Tobita, S.; Shizuka, H.; Nishimura, J. *J. Am. Chem. Soc.* **1996**, *118*, 1006.
(45) Frisch, M. J.; Trucks, G. W.; Schlegel, H. B.; Gill, P. M. W.; Johnson, B. G.; Robb, M. A.; Cheeseman, J. R.; Keith, T. A.; Petersson, G. A.; Montgomery, J. A.; Raghavachari, K.; Al-Laham, M. A.; Zakrzewski, V. G.; Ortiz, J. V.; Foresman, J. B.; Cioslowski, J.; Stefanov, B. B.; Nanayakkara, A.; Challacombe, M.; Peng, C. Y.; Ayala, P. Y.; Chen, W.; Wong, M. W.; Andres, J. L.; Replogle, E. S.; Gomperts, R.; Martin, R. L.; Fox, D. J.; Binkley, J. S.; Defrees, D. J.; Baker, J.; Stewart, J. P.; Head-Gordon, M.; Gonzalez, C.; Pople, J. A. *Gaussian 94, Revision A.1*; Gaussian Inc.: Pittsburgh, PA, 1995.

(46) Zadorozhnyi, B. A.; Ishchenko, I. K. *Opt. Spectrosc.* (Engl. Transl.) **1965**, *19*, 306.
(47) Hunsberger, I. M. *J. Chem. Phys.* **1950**, *72*, 5626.
(48) Pouchert, C. J.; Behnke, J. *The Aldrich Library of 13C and 1H FT NMR Spectra*, 1st ed.; Aldrich Chem. Co.: WI, 1975.
(49) Badger, R. M.; Bauer, S. H. *J. Chem. Phys.* **1937**, *5*, 839. Badger, R. M. *J. Chem. Phys.* **1940**, *8*, 288.
(50) Sandros, K. *Acta Chem. Scand., Ser. A* **1976**, *30*, 761.
(51) Sundaralingam, M.; Jensen, L. H. *Acta Crystallogr.* **1965**, *18*, 1053.
(52) Braslavsky, S. E.; Heihoff, K. In *Handbook of Organic Photochemistry*; Scaiano, J. C., Ed.; CRC Press: Boca Raton, FL, 1989; Vol. 1, p 327.
(53) Braslavsky, S. E.; Heibel, G. E. *Chem. Rev.* **1992**, *92*, 1381.
(54) Terajima, M.; Azumi, T. *Chem. Phys. Lett.* **1987**, *141*, 237.
(55) Itoh, M.; Fujiwara, Y.; Sumitani, M.; Yoshihara, K. *J. Phys. Chem.* **1986**, *90*, 5672.
(56) Shizuka, H.; Machii, K.; Higaki, Y.; Tanaka, M.; Tanaka, I. *J. Phys. Chem.* **1985**, *89*, 320.
(57) McMorrow, D.; Kasha, M. *J. Phys. Chem.* **1984**, *88*, 2235.
(58) Kasha, M. *J. Chem. Soc., Faraday Trans. 2* **1986**, *282*, 2379.
(59) (a) Arai, T.; Tobita, S.; Shizuka, H. *J. Am. Chem. Soc.* **1995**, *117*, 3968. (b) Arai, T.; Tobita, S.; Shizuka, H. *Chem. Phys. Lett.* **1994**, *223*, 521.
(60) Kimura, Y.; Yamamoto, M.; Tobita, S.; Shizuka, H. *J. Phys. Chem. A* **1997**, *101*, 459.
(61) Catalán, J.; Palomar, J.; De Paz, J. L. G. *Chem. Phys. Lett.* **1997**, *269*, 151.
(62) (a) Brewer, W. E.; Martinez, M. L.; Chou, P.-T. *J. Phys. Chem.* **1990**, *94*, 1915. (b) Al-Soufi, W.; Grellmann, K. H.; Nickel, B. *Chem. Phys. Lett.* **1990**, *174*, 609. (c) Stephan, J. S.; Rodríguez, C. R.; Grellmann, K. H.; Zachariasse, K. A. *Chem. Phys.* **1994**, *186*, 435. (d) Stephan, J. S.; Grellmann, K. H. *J. Phys. Chem.* **1995**, *99*, 10066.
(63) Konijnenberg, J.; Huizer, A. H.; Varma, C. A. G. O. *J. Chem. Soc., Faraday Trans. 2* **1988**, *84*, 363.
(64) Yasunaga, T.; Tatsumoto, N.; Inoue, H.; Miura, M. *J. Phys. Chem.* **1969**, *73*, 477.
(65) van der Burgt, M. J.; Jansen, L. M. G.; Huizer, A. H.; Varma, C. A. G. O. *Chem. Phys.* **1995**, *201*, 525.
(66) Kitamura, M.; Baba, H. *Bull. Chem. Soc. Jpn.* **1975**, *48*, 1191.
(67) Lim, E. C. *J. Phys. Chem.* **1986**, *90*, 6770.
(68) Nagaoka, S.; Nagashima, U. *Trends Phys. Chem.* **1997**, *6*, 55.